This is a preprint, the final version is subject to change, of the American Mineralogist (MSA)
Cite as Authors (Year) Title. American Mineralogist, in press.
DOI: https://doi.org/10.2138/am-2019-6869CCBYNCND

Ms 6869R1

Synthesis of Pigeonites for Spectroscopic Studies

Donald H. Lindsley[1]*, Hanna Nekvasil[1], and Timothy D. Glotch[1]

[1]Department of Geosciences, ESS Building, 100 Nicholls Road, Stony Brook University 11794-2100

*Email: donald.lindsley@stonybrook.edu , hanna.nekvasil@stonybrook.edu , timothy.glotch@stonybrook.edu

ABSTRACT

Pigeonite ($P2_1/c$ clinopyroxene) crystallizes in a variety of terrestrial and extraterrestrial rocks. However, because it breaks down ("inverts") in slowly cooled rocks, bulk natural samples of pigeonite from coarse-grained rocks are not available. We have synthesized eight samples of pigeonite with compositions of Wo_8 and Wo_{10} (where Wo (mol %) = $100Ca/(Ca + Mg + Fe^{2+})$) and X ranging from 20 to 60 (where X = $100Fe^{2+}/(Mg + Fe^{2+})$). These samples are suitable for spectroscopic and other studies that require bulk samples. Because of relatively fine grain size (mainly 5-50 μm) and slight grain-to-grain variation in composition, they are generally not suitable for studies requiring individual crystals. We will make samples available for appropriate investigations, especially if the techniques used are non-destructive and the samples can be returned after use.

INTRODUCTION

Pigeonite (i.e., clinopyroxene containing approximately 10% Wo (where the amount of Wo (atomic %) = $100Ca/(Ca + Mg + Fe^{2+})$) is reported from terrestrial, lunar, and planetary

samples (e.g., Basaltic Volcanism Study Project, 1981, p. 65, 184, 224). It forms in a variety of igneous and high-temperature metamorphic rocks, but survives as a discrete phase almost exclusively in rapidly cooled, fine-grained lavas. This is because pigeonite has a minimum thermal stability temperature below which, upon slow cooling, it breaks down ("inverts") to an intergrowth of augite lamellae in an orthopyroxene host - the so-called "inverted pigeonite" texture. Since pigeonite does not survive as a discrete phase in plutonic rocks and it is tedious to separate pigeonite grains from the fine-grained lavas in which they do survive, we lack natural pigeonite for measurements that require bulk samples. To remedy this, we have synthesized eight samples of pigeonite to serve as standards for spectroscopic and other studies.

Synthesis of pigeonite is complicated by several characteristics of phase equilibria in the pyroxene quadrilateral. Pigeonite synthesis must take place within its stability field, that is, above the temperature of its minimum thermal stability (e.g., Fig. 6 of Davidson and Lindsley, 1985) but below the solidus temperature in the pure $Ca_2Si_2O_6$-$Mg_2Si_2O_6$-$Fe_2Si_2O_6$ system (Fig. 4b of Huebner and Turnock, 1980; our Fig. 1). Thus, for a given X (X = $100Fe^{2+}/(Fe^{2+} + Mg)$ molar), there is a relatively narrow temperature window for successful synthesis. Furthermore, as both the minimum pigeonite stability and solidus temperatures decrease with increasing X, this window shifts with composition. Much early work concentrated on making pigeonite in the Fe-free (Kushiro, 1969; Yang, 1973; Schweitzer, 1982; Tribaudino et al. 2002) and Mg-free (Lindsley, 1981) joins. Turnock et al. (1973) reported synthesis of pigeonite at a wide variety of X, and listed several techniques for synthesis. They used their Method 1 (controlled-gas, quench furnace, one atmosphere) to make pigeonites with X ranging from 20 to 60, and their Method 5 (hydrothermal synthesis at 2 GPa) for pigeonite with X = 75 (because pigeonite of that composition lies in the

"Forbidden Zone" and is not stable at one bar, e.g., Lindsley, 1983). Neither method, however, is well suited for making gram-quantities of pigeonite, so we used a modification of their Method 2: synthesis in sealed, evacuated silica-glass tubes, to allow us to process 1 to 3 grams of material in each tube. We aimed to make ~ 5 grams of each composition, with Wo values of 8 and 10, and X ranging from 20 (few natural pigeonites are more magnesian than this) to 60 (near the edge of the "Forbidden Zone" and thus near the limit for synthesis at low pressure).

SYNTHESIS DETAILS

Starting materials.

All initial mixes were made from stoichiometric quantities of dried $CaSiO_3$, MgO, SiO_2 (quartz), Fe_2O_3, and Fe° sponge. We used hematite and iron sponge as the source of FeO because stoichiometric FeO is not stable. We measured the amount of oxygen in the Fe° sponge (see p. 52 of Turnock et al., 1973; also Supplementary Materials) and adjusted the amount of hematite used accordingly to yield the desired bulk FeO composition. All components except the Fe° sponge were ground together under ethanol for several hours in an automatic agate mortar; to minimize oxidation, the sponge was added only for the last 30-40 minutes of grinding.

Previous experience had shown that placing the original starting mix directly into the pigeonite stability field yields pigeonite riddled with inclusions of intermediate phases (augite, olivine, and silica); and because those intermediate phases were "armored" within pigeonite, reaction among them became extremely slow. We avoided most of that difficulty by "pre-reacting" the starting materials at 900-920 ºC, a temperature range below the minimum stability of pigeonite (details in Supplementary materials). The pre-reacted starting material for the pigeonite synthesis consisted of crystalline augite, olivine, and quartz.

Final synthesis.

Pre-reacted materials were packed into iron capsules machined to 2 to 4 cm in length with snugly fitting lids from medium-purity (99.6 to 99.95%) 1/4 inch (6.35 mm) OD rod. The loaded capsules were placed in 7 mm ID silica-glass tubes, dried under vacuum at 800º C for 10 minutes using an iron "oxygen getter" (Fe° sponge) placed in the tubes at ~600 ºC to prevent oxidation, and the tubes were then sealed under vacuum. We used two heating approaches for the synthesis. The first involved holding the sample at a fixed temperature below the solidus for direct synthesis in the solid state. The second approach involved partially melting the sample at ~25-50 ºC above the solidus temperature, then cooling it slowly to below the solidus temperature, and finally holding the sample at that lower temperature, with the goal of using the presence of melt to speed up reaction and to grow larger crystals. Unfortunately, most samples treated using this second approach were strongly zoned, with low-Ca, high-Mg cores mantled by rims close to the target composition. Only one sample treated in this way (Wo_{10} X=60 T) was sufficiently homogeneous to be acceptable (Fig. 2). (Samples are named by the target composition plus a letter (A, B, etc.) designating the sequence of that sample in the synthesis attempts for that composition.)

All but one sample (Wo_8 X=40 E) underwent more than one stage of "final" synthesis: the products of previous attempts were re-heated (usually with intermediate grinding) to produce more nearly homogeneous materials. Details are in Table S1, Supplementary materials. Especially for more magnesian compositions that required higher temperatures, run durations were nerve-wracking compromises between the desire to maximize reaction time and the knowledge that the enclosing silica-glass tubes would eventually fail because of softening and/or devitrification. Because of the recycling and associated losses of material (when the silica-glass tubes failed and samples within them became oxidized), the samples reported here fall short of the

93 5-gram target by varying amounts.

94

95 **Characterization of materials**

96 We characterized the synthesis products optically (both under a binocular microscope, and
97 immersed in refractive-index oil under a petrographic microscope), with powder X-ray diffraction;
98 and by electron microprobe. Optical examination showed mainly pigeonite; small amounts of a
99 silica phase; rare olivine inclusions (where noted in Table 1); and residual quenched melt (one
100 sample). Because syntheses were performed in iron capsules, *all samples contain iron metal* **(**<0.1
101 to 0.9 wt% Fe°)**,** as inclusions and/or discrete grains.

102 **X-ray diffraction.** We used Stony Brook's Rigaku Miniflex system with Cu radiation,
103 scanning from 18 to 128º 2θ for our powder XRD analyses. Diffraction data were processed with
104 **Match! 3** (Putz, 2016) to identify phases, compute their proportions, and to refine the pigeonite
105 cell parameters (Table 1). Pigeonite dominated in the assemblage produced; however, most
106 samples also showed small amounts (0.5 to 2 wt%) of unreacted silica. Although tridymite is
107 considered the stable polymorph of SiO_2 at the conditions of synthesis, only one sample showed
108 tridymite. Mg-rich compositions (which required higher synthesis temperatures) produced mainly
109 cristobalite; Fe- rich ones contained quartz, presumably inherited from the starting material.

110 Our unit-cell parameters (Table 1) agree moderately well with values predicted by the
111 equations of Morrison et al. (2018) (Pigeonite: $P2_1/c$ in box, top of their p. 852). Although there is
112 some variation, their predicted values average 0.008Å lower than our measured values for a;
113 -0.006Å lower for b; 0.0004Å lower for c; and 0.09º higher for β. Measured and calculated values
114 are shown in Table S2 (Supplementary Materials).

115 **Microprobe analysis**. The goal for quantitative compositional analysis was to report the

116 widest observed range of compositions. Standards used in EMPA were anorthite for Ca, San
117 Carlos olivine for Mg; fayalite for Fe, and Lake County plagioclase for Si. Analysis conditions
118 were 1 μm nominal beam size, 15KeV accelerating voltage and 20nA beam current. Because the
119 samples are saturated with iron metal, we assume that virtually all the iron structurally in the
120 pigeonite is Fe^{2+}. Owing to the small grain size of most samples, most analyses aimed for the
121 centers of the grains and the search for minor phases and zoning within pigeonite was restricted to
122 backscattered electron imaging. We report (Fig. 2; Table S3, Supplementary Materials) all
123 analyses that totaled 98-102 wt% and approached $M_2Si_2O_6$ stoichiometry (Si 1.98 -2.02; divalent
124 cations 1.98 -2.02 per 6 oxygens). For three samples (Wo8 X=30 G; Wo8 X=30 F; Wo8 X=40 E)
125 we had to accept sums lower than 98%, in part because of fine grain size. Most analyses for most
126 samples cluster close to (but are slightly more Mg-rich than) the target compositions. Mg-rich
127 outliers most likely reflect zoning within pigeonite; those with higher Fe and lower Ca than the
128 intended bulk composition probably overlap onto olivine inclusions (olivine that coexists with
129 pigeonite has higher values of X; see Fig. 1); and those with higher Ca and higher Fe almost
130 certainly represent overlap with quenched melt. Although the final temperatures of synthesis were
131 always below the solidus (Fig. 1) the pre-reacted starting material was not the stable assemblage at
132 T, therefore, metastable melting was a possibility, and some of this melt may have survived the
133 prolonged soak at the subsolidus T. Please note that because we deliberately searched for and
134 report outlier compositions, the **range** of compositions in Fig. 2 is almost certainly NOT
135 representative of the **bulk composition** of the sample, which is best approximated by the clustered
136 analyses. That conclusion is bolstered by the relatively sharp peaks in the X-ray diffraction
137 patterns.
138

This is a preprint, the final version is subject to change, of the American Mineralogist (MSA)
Cite as Authors (Year) Title. American Mineralogist, in press.
DOI: https://doi.org/10.2138/am-2019-6869CCBYNCND

IMPLICATIONS

Because bulk samples of natural pigeonites are not available, synthetic samples are needed for a variety of studies. However, synthesis of gram-quantities of pigeonite remains difficult. The eight samples reported here are products of the most successful of more than 125 synthesis attempts over several years. Potential users of these samples should be aware of the within-sample variations; the samples should be used for studies on **bulk** samples. As any individual grain may deviate considerably from the nominal composition, we do not recommend using individual crystals unless each crystal has been analyzed by microprobe.

Those who wish to obtain samples for specific studies should contact T. D. Glotch, (timothy.glotch@stonybrook.edu), stating the composition(s) desired, which measurements will be made; optimum and minimum quantities needed; and whether the sample(s) can be returned undamaged and uncontaminated after use. Requesters should take into account (i) the widely varying amounts available for each sample, (ii) that some samples are more nearly uniform in composition than others, and (iii) that there are variations in grain size. Preference will be given to those who will use nondestructive techniques. Please note that the sample names include both the target compositions **and** the letter (e.g., A, B, C) that uniquely designates the particular sample. (For example, the sample name Wo_{10} X= 60 T implies that there are at least 19 other samples (A...S) of that target composition! The T is essential for identifying that sample.) *The letter designator must be retained in all reports that use the sample.*

ACKNOWLEDGMENTS

This paper is dedicated to the fond memory of Allan Charles Turnock (1930-2018), colleague and

close friend of DHL since student days. Samples were analyzed using the Cameca SX-100 probe at the American Museum of Natural History (New York). We thank Nicholas DiFrancesco, Douglas Schaub, and Tristan Catalano for their careful work in probing these challenging samples, and Adrian Fiege for helping them. Alexandra Sinclair contributed to early stages of the project. We thank Mario Tribaudino, Stephen Huebner, and an anonymous reviewer for their timely and helpful reviews. This work was supported by the RIS^{4}E node of NASA's Solar System Exploration Research Virtual Institute (TDG) and by NSF grant EAR1725212 (HN).

REFERENCES CITED

Basaltic Volcanism Study Project (1981) Basaltic Volcanism on the Terrestrial Planets. New York: Pergamon Press, 1286 pp.

Davidson, P.M., and Lindsley, D.H. (1985) Thermodynamic analysis of quadrilateral pyroxenes. Part II: Model calibration from experiments and applications to geothermometry. Contributions to Mineralogy and Petrology 91, 390-404.

Huebner, J.S., and Turnock, A.C. (1980) The melting relations at 1 bar of pyroxenes composed largely of Ca-, Mg-, and Fe-bearing components. American Mineralogist 65, 225-271.

Kushiro, Ikuo (1969) The system forsterite-diopside-silica with and without water at high pressures. American Journal of Science 267-A (Schairer Volume), 269-294.

Lindsley, D.H. (1981) The formation of pigeonite on the join hedenbergite-ferrosilite at 11.5 and

15 kbar: Experiments and a solution model. American Mineralogist 66, 1175-1182.

Lindsley, D.H. (1983) Pyroxene Thermometry. American Mineralogist 68, 477-493.

Morrison, S.M., Downs, R.T, Blake, D.F., Prabhu, A., Eleish, A., Vaniman, D.T., Ming, D.W., Rampe, E.B., Hazen, R.M., Achilles, C.N., and others (2018). Relationships between unit-cell parameters and composition for rock-forming minerals on Earth, Mars, and other extraterrestrial bodies. American Mineralogist 103, 848-856.

Putz, H. (2016) Match! - Phase Identification from Powder Diffraction - Version 3, Crystal Impact - Dr. H. Putz & Dr. K. Brandenburg GbR, Kreuzherrenstr. 102, 53227 Bonn, Germany, http://www.crystalimpact.com/match .

Schweitzer, E.J. (1982) The reaction pigeonite = $diopside_{ss}$ + $enstatite_{ss}$ at 15 kbars. American Mineralogist 67, 54-58.

Tribaudino, M., Nestola, F., Cámara, F., and Domeneghetti, M. C. (2002) The high temperature $P2_1/c$-$C2/c$ phase transition in Fe-free pyroxene ($Ca_{0.15}Mg_{1.85}Si_2O_6$): structural and thermodynamic behavior. American Mineralogist, 87, 648-657.

Turnock, A.C., Lindsley, D.H., and Grover, J.E. (1973) The synthesis and unit-cell parameters of Ca-Mg-Fe pyroxenes. American Mineralogist 58, 50-59.

Yang, H.-Y. (1973) Crystallization of iron-free pigeonite in the system anorthite-diopside-

enstatite-silica at atmospheric pressure. American Journal of Science 273, 488-497.

Figure Captions

Figure 1. Solidus diagram for Ca-Mg-Fe^{2+} pyroxenes at one atm. (adopted from Huebner and Turnock , 1980; their Fig. 4b), showing the approximate pigeonite field and the target compositions for our work (open circles). Wo (mol%)= $Ca_2Si_2O_6$, or $100Ca/(Ca + Mg + Fe^{2+})$; X = $100Fe^{2+}/(Mg + Fe^{2+})$(atomic %); En = $Mg_2Si_2O_6$; Fs = $Fe_2Si_2O_6$; Di = $CaMgSi_2O_6$; Hd = $CaFeSi_2O_6$; Opx = orthopyroxene; Ol = olivine; S = silica phase (tridymite, cristobalite, or quartz). We omit labels for the complex region near Hd and Fs. Note that olivine has higher X than the coexisting pigeonite, as shown by the composition of olivine coexisting with pigeonite at the solidus.

Figure 2. Portion of the pyroxene quadrilateral showing target compositions (open circles) and microprobe analyses (solid points; Supplemental Table S2) of the samples. All analyses with close to $(Mg+Fe+Ca)_2Si_2O_6$ stoichiometry (Si = 1.98 to 2.02; Ca + Mg + Fe (+ Mn) = 1.98-2.02) are plotted. MnO (generally < O.6 and more commonly < 0.3 wt. %) was added to FeO to form Fs component. Black symbols and text refer to Wo_{10} samples; gray to Wo_8. We deliberately searched for and report outlier compositions to show diversity of grain compositions. For this reason the bulk compositions of the samples are best represented by the clusters of analyses near the target compositions, not an average of the points shown. See text for interpretation of outlier points. Components as in caption to Fig. 1.

Table 1. Synthesized pigeonites.

Target Comp.[a]	Sample Letter	Synthesis Temp. (°C)	~Grams available	Grain size (µm)	Yield (wt%)		CELL PARAMETERS ($P2_1/c$)[c]				
					Pigeonite	Other phases[b]	a (Å)	b (Å)	c (Å)	β (degrees)	V (Å^3)
Wo8 X=20	G	1225	0.4	25-50	98	cr (2); ol (tr)	9.6774(4)	8.8881(4)	5.2197(2)	108.4808(36)	425.815(6)
Wo10 X=20	F	1225	4	5-50	>99	cr (0.5); ol (tr)	9.6851(3)	8.8907(3)	5.2263(2)	108.439(3)	426.918(7)
Wo8 X=30	F	1225	0.8	5-10	>99	cr (0.7)	9.6832(4)	8.9047(3)	5.2242(2)	108.521(3)	426.985(8)
Wo10 X=30	I	1225	2.6	5-50	>99	trid (0.6)	9.6918(5)	8.9084(4)	5.2300(2)	108.487(4)	428.246(7)
Wo8 X=40	E	1185	4	5-10	>99	qtz (0.9)	9.6960(4)	8.9315(3)	5.2322(2)	108.553(3)	429.564(7)
Wo10 X=40	K	1186	1.6	5-30	>99	cr (0.6); ol (tr)	9.7058(4)	8.9363(3)	5.2393(2)	108.496(3)	430.950(8)
Wo8 X=55	D	1075	0.37	5-10	>99	qtz (0.6); gl (tr)	9.7082(5)	8.9677(4)	5.2403(3)	108.545(4)	432.528(7)
Wo10 X=60	T	1260;1144	0.7	80-120	>99	gl (tr)	9.724(1)	8.987(1)	5.2492(9)	108.38(2)	435.33(2)

"Note:" Because syntheses were done in Fe° capsules, all samples contain metallic iron. Match! reports <0.1 to 0.9 wt% Fe°. Details of each synthesis are in Supplementary materials.

[a]Wo = 100Ca/(Ca+Mg+Fe). X = 100Fe/(Mg+Fe) atomic.

[b]cr - cristobalite; trid - tridymite; qtz - quartz; ol - olivine; gl - glass or quenched melt; tr - trace (seen optically or inferred from outlier probe analyses).

[c]Values in () show 1σ uncertainty in last significant figure, calculated by multiplying the formal uncertainty of the refinement by the Berar "Score",

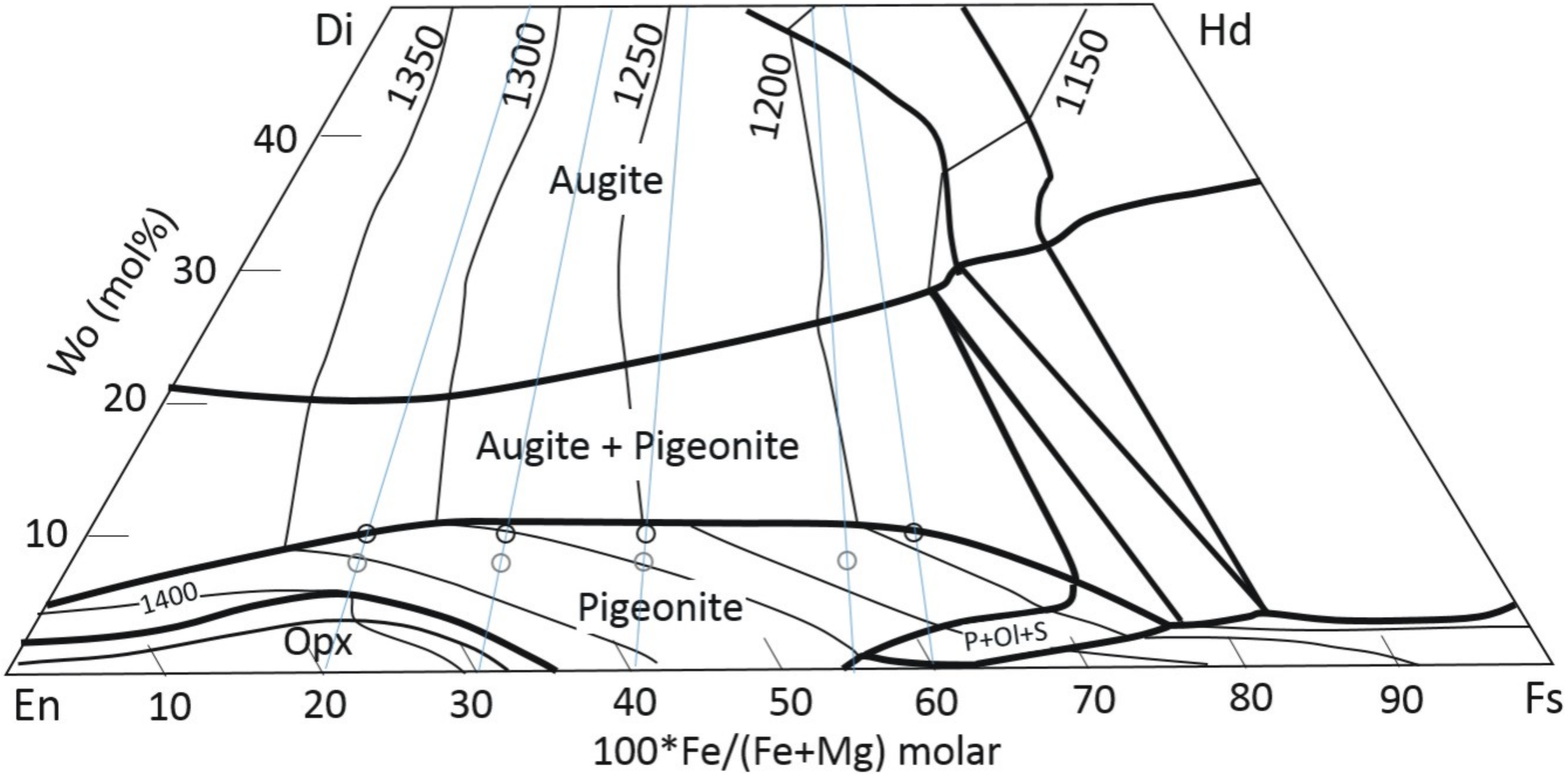

Figure 1. Lindsley et al.

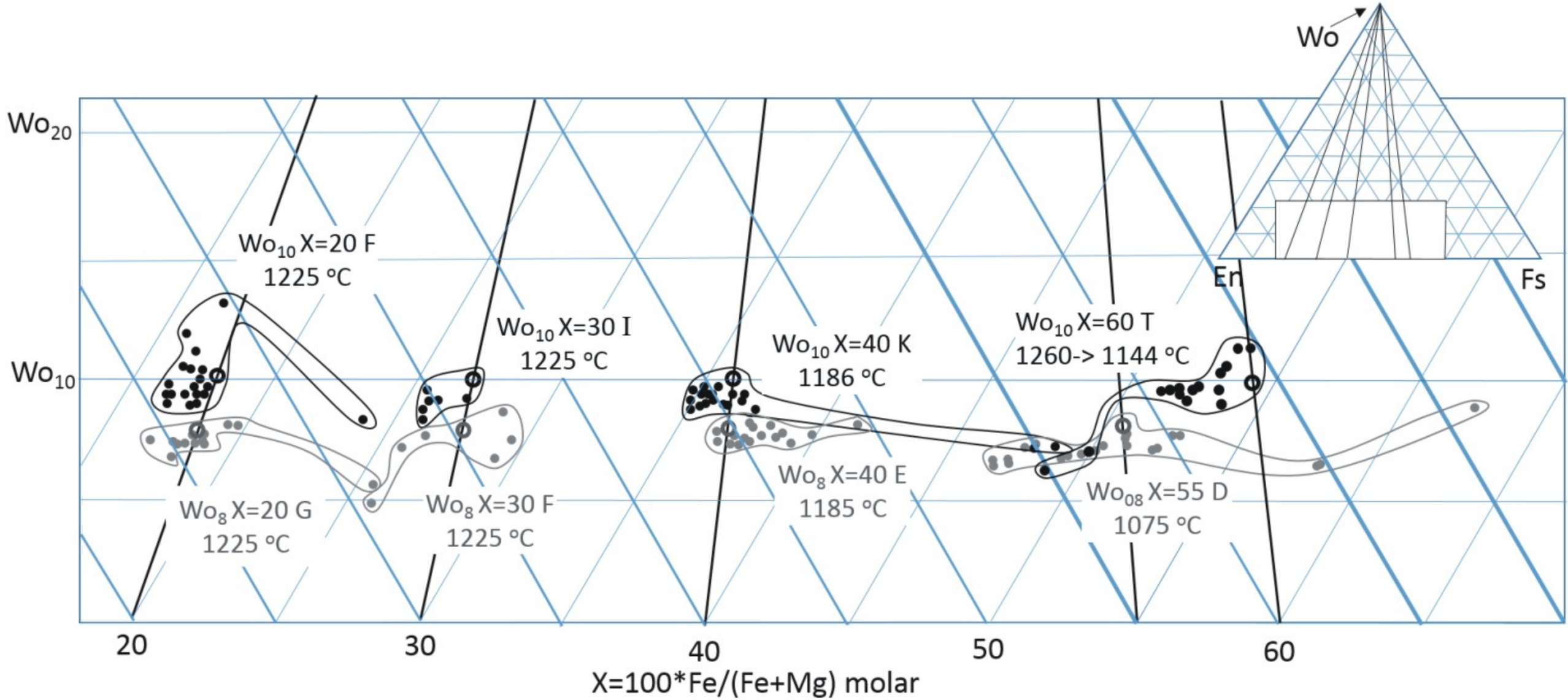

Figure 2 Lindsley et al.